An Accurate Model of Multi-Type Overcurrent Protective Devices Using Eigensystem Realization Algorithm and Practice Applications

Chao-Yuan Cheng[†] and Feng-Jih Wu*

Abstract – Accurate models of the characteristics of typical inverse-time overcurrent (OC) protective devices play an important role in the protective coordination schemes. This paper presents a novel approach to determine the OC protective device parameters. The approach is based on the Eigensystem Realization Algorithm which generates a state space model to fit the characteristics of OC protective devices. Instead of the conventional characteristic curves, the dynamic state space model gives a more exact fit of the OC protective device characteristics. This paper demonstrates the feasibility of decomposing the characteristic curve into smooth components and oscillation components. 19 characteristic curves from 13 typical and 6 non-typical OC protective devices are chosen for curve-fitting. The numbers of fitting components required are determined by the maximum absolute values of errors for the fitted equation. All fitted equations are replaced by a versatile equation for the characteristics of OC protective devices which represents the characteristic model of a novel flexible OC relay, which in turn may be applied to improve the OC coordination problems in the sub-transmission and distribution systems.

Keywords: Curve fitting, Eigensystem realization algorithm, Novel flexible overcurrent relay, Multi-function equation, Overcurrent protective device.

1. Introduction

At present, power generation systems which fault currents at buses do not differ much from those at transmission lines that may be due to there are few large generators connected directly to their sub-transmission systems and distribution systems. Therefore, makes low cost, reliable, and easily coordinated inverse-time electromechanical (EM) overcurrent (OC) relays suitable protective coordination devices in the sub-transmission and distribution systems. Meanwhile some older relays have been replaced by new digital ones, there are still many EM OC relays in service. Besides, due to their low cost and effectiveness as EM OC relays, power fuses are commonly utilized to protect for motors, capacitors, and transformers, or as safeguard between the utility and loads in distribution systems.

Based on the operation principle of the EM OC relay will introduce an electric current into the coil of an electromagnet which produces the eddy currents with phase differences. Thus, induction torque will be generated on the rotation disc of the relay at moment. The proper contact closing time can be set by adjusting the distance between the fixed and the movable contacts to achieve protective coordination between the upstream and the downstream relays. However, due to the mechanical nature of the relay, there are inertial and frictional effects.

Therefore, unlike a digital OC relay [1], it is not possible to model the characteristic of an EM OC relay accurately by a single equation. A power fuse is made of metallic material that melts under high temperature. As the thermal effect of the Fault current builds up, the metallic material melts down to interrupt the fault current. Therefore, neither is it possible to accurately model the characteristic curve of a power fuse by a single equation.

Researchers have always been interested in curve fitting EM OC relay characteristics [2] to facilitate protective coordination in power systems. After the introduction of the digital OC relays, better curve-fitting of EM OC relay characteristics [3-6] is even more important for proper protective coordination. On the other hand, the curve-fitting of power fuse characteristics is relatively rare in the reference [7] due to their location and voltage level in the power systems.

Because the characteristics of EM OC relays and power fuses cannot be accurately represented by a single equation, it is difficult for them to coordinate with other OC protective devices. On the other hand, because digital relays [5] are programmable, flexible and accurate, they are now widely used in power systems.

There are several different types of inverse-time EM OC relays: short inverse, long inverse, definite inverse, moderately inverse, inverse, very inverse, and extremely inverse [8]. Relays with different inverse-time characteristics are suitable for different applications, e.g., a CO2 (short inverse) OC relay is suitable for protection of bus. Families of characteristic curves of a certain type of relays with different time dial setting (*TDS*) are generally provided in

† Corresponding Author: Department of Electrical Engineering, Tam King Road, Tamsui District, New Taipei City, 25135 Taiwan, R.O.C. (cyj@mail.sju.edu.tw)
* Department of Electrical Engineering, Tam King Road, Tamsui District, New Taipei City, 25135 Taiwan, R.O.C. (roger@mail.sju.edu.tw)

the manuals by the manufacturers. These characteristics, as well as those of the digital OC relays and power fuses, are all piecewise nonlinear continuous smooth descending curves on a log-log coordinates. Such relays and fuses are called the typical OC protective devices.

Most of the literatures about EM OC relay characteristics curve-fitting show the absolute values of errors [6, 9-10], while some show the averages of absolute values of errors [9, 11]. However, only a few studies show the maximum absolute values of percentage errors which are more accuracy-related [11], and no studies show the maximum absolute values of errors which are the most accuracy-related to curve-fitting of relay characteristics. For the others, for EM OC relays at small values of M (multiples of tap value current), e.g., 1.3-3.0, the relay operating time changes nonlinearly and drastically, and only one study [11] shows the curve-fitting results in this range of M values. To demonstrate the accuracy of the proposed curve-fitting method, this current study not only shows all the maximum absolute values of errors, maximum absolute values of percentage errors, averages of absolute values of errors and averages of absolute values of percentage errors, but also considers smaller values of M where the relay operating time changes nonlinearly and drastically. To even better accuracy, this study reduces the maximum absolute values of errors not only to less than an alternating current cycle but also to the range of a few ms (milliseconds), as opposed to 3 cycles in [3] or 2 cycles in [10].

This paper applies the Eigensystem Realization Algorithm (ERA) [12-14] method to determine the parameters of the OC protective device characteristic. The ERA method produces a digital state space model which, because of its dynamic nature, gives a more exact fit for both the typical and non-typical OC protective device characteristics. By applying the proposed ERA method, the OC protective device characteristics are decomposed into various smooth and oscillatory wave components which are related to the eigenvalues of the identified state space matrix [13]. The eigenvalues are the poles of the system transfer function and the natural frequencies of the network [14], and they represent the dynamic characteristics of the wave components.

IEEE and IEC normal standard inverse-time digital OC relay characteristic models [5, 15] are obtained by a simple equation, and applying the ERA accurately to curve-fit the characteristics of OC protective devices or any such curves can be accomplished by a standard equation. A customized OC relay with an equation such as one proposed by this study can be used to adjust any protection coordination curve in the system protection coordination design. ERA was merely applied in [16] to curve-fit the characteristics of EM OC relays. The current study applies ERA not only to various protective devices but also to obtain an accurate model of multi-type OC protective devices and introduce several practical applications.

There are 13 typical OC protective devices in this study:

four EM OC relays [8, 17], three IEEE normal standard digital OC relays [5], four IEC normal standard digital OC relays [15] and two power fuses [18]. The others are 2 non-typical OC protective devices with special-purpose characteristic curves and 4 non-typical OC protective devices with fixed slope characteristic curves on a log-log coordinates. All of these devices are called OC protective devices. 19 characteristic curves are selected to be curve-fitted by the proposed ERA method to obtain a multi-function equation to model the characteristics of the OC protective devices. The equation can be used as the model of a novel flexible relay to solve the coordination problems in power systems.

MATLAB programs are developed in this study to plot the characteristic curves. The rest of this paper is organized as follows. Typical OC protective device are described in Section 2. The proposed ERA method and the mathematics are outlined in Section 3. Five case studies are presented in Section 4. The simulation results and practical applications in power systems are discussed in Section 5 and 6, respectively. The conclusions is in Section 7.

2. Models of Typical OC Protective Devices

EM OC relays, digital OC relays and power fuses are typical OC protective devices for faults in the sub-transmission and distribution systems. The manufacturers provide the characteristics in the manuals as two-dimensional curves with M or fault current the abscissa and operating time the ordinate.

2.1 Electromechanical Overcurrent (EM OC) Relay

The characteristic of an EM OC relay is determined by its magnetic circuit design. Conventional models of EM OC relay characteristics are as follows:

2.1.1 Exponential and Polynomial Forms

Various forms represented by exponential and polynomial equations are summarized and recommended by the IEEE Committee [3], e.g., Eqs. (1)-(5) below, for EM OC relay characteristic curve-fitting. In some studies [6, 10-11] that apply numerical methods to determine the best coefficients of the curve-fitting equations, the maximum absolute values of percentage errors are as large as 15% [11], so there is still much room for improvement.

$$t = Y \times TDS / (M^p - 1) + Z = Y \times TDS / ((i/I_n)^p - 1) + Z \quad (1)$$

$$t = a_0 + a_1 \times TDS + a_2 \times TDS^2 + a_3 \times TDS^3 + \cdots \quad (2)$$

$$t = b_0 + b_1 / (M - 1) + b_2 / (M - 1)^2 + b_3 / (M - 1)^3 + \cdots \quad (3)$$

$$t = c_0 + c_1 / \log M + c_2 / (\log M)^2 + c_3 / (\log M)^3 + \cdots \quad (4)$$

$$t = d_0 + d_1 \times TDS + d_2 \times TDS / (M - 1)^2$$

$$+d_3 \times TDS^2 / (M-1) \quad +d_4 \times TDS^2 / (M-1)^2$$
$$+d_5 \times TDS / (M-1)^3 + d_6 \times TDS^2 / (M-1)^4 \qquad (5)$$

$$t = TDS \times \left(F / (M^p - 1) + G \right) + H \qquad (6)$$

where

t: operating time
TDS: time dial setting
i: fault current on the secondary side of the CT
I_n: current tap setting
M:=multiples of tap value current, $M = i / I_n$
$F, G, H, Y, Z, a_n, b_n, c_n, d_n, p$: constants

2.1.2 Characteristic equation simulation

Take the characteristic curves of the ABB's EM OC relay CO-8 [8] as an example. The recommended values of F, G, H and p in Eq. (6) are 8.9341, 0.17966, 0.028 and 2.0938, respectively, in [19]. The actual and the fitting characteristic curves are plotted in Figure 1 as solid black curves and dotted curves, respectively, with TDS settings of 0.5, 2, 5 and 10. The averages of absolute values of errors of the 488 sampling operating times for TDS settings 0.5, 2, 5 and 10 are 99.95, 189.18, 382.16 and 449.94 ms, respectively. These fitting curves differ considerably from the actual characteristic curves and cannot be used directly as a good replacement.

Consider the case in [20] in which the TDS settings in Eq. (6) are modified to 0.3, 1.5, 4 and 8.7, while their manufacture data counterparts remain the same as 0.5, 2, 5 and 10, respectively, which are plotted as solid grey curves
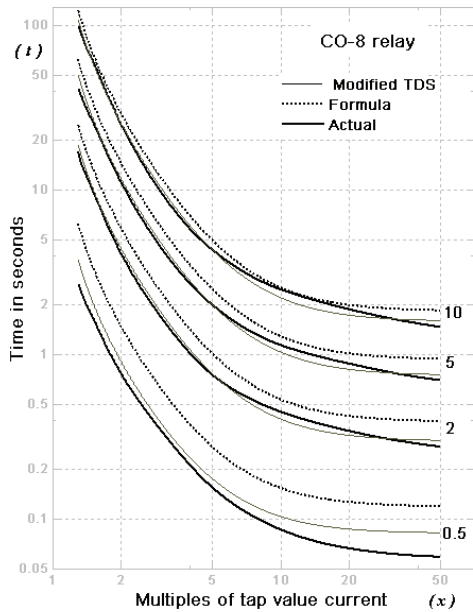

Fig. 1. The actual (solid black), fitting (dotted black) and modified fitting (solid grey) characteristic curves by Eq. (6) for the CO-8 relay.

in Fig. 1. The averages of absolute values of errors of the four sets of 488 sampling operating times taken between the modified fitting curve and the actual characteristic curve are 28.64, 32.54, 90.97 and 168.74 ms, respectively. Although this modified Eq. (6) is much more accurate, it is still not good enough to represent the actual characteristic curves provided by the manufacturer.

2.1.3 Data Base Method

The values of M and the corresponding operating times are stored directly [3-4]. This type of model is commonly used today, but requires large data storage. Because the relay characteristics cannot be modeled by a single equation, interpolation is usually applied to estimate data points not stored.

2.1.4 Artificial Intelligence Techniques

Researchers are applying more Artificial Neural Network and Fuzzy Model techniques [6, 9] to optimal curve fitting. Among these approaches, the ANFIS models developed by M. Geethanjali [9] show promising results. However, its maximum absolute value of errors is 28 ms and its average absolute value of errors is 11.8 ms, so there is still some room for improvement.

2.2 Digital OC relays

Eq. (6) is obtained by modifying Eq. (1) in [19] for simulation. The IEEE normal standard inverse-time digital OC relay characteristic model is obtained by letting $H = 0$ [5], and the IEC normal standard inverse-time digital OC relay characteristic model is obtained by letting both $H = 0$ and $G = 0$ [15]. They are rewritten as Eqs. (7) and (8). Depending on load patterns, a flexible and accurate characteristic curve can be determined by adjusting the values of TDS β γ and ε in the equation. Equations (7) and (8) are widely used for typical OC protective devices in new or rebuilt power systems.

$$t(M) = TDS \times \left(\beta / \left(M^\gamma - 1 \right) + \varepsilon \right) \qquad (7)$$

$$t(M) = TDS \times \beta / \left(M^\gamma - 1 \right) \qquad (8)$$

where

$\varepsilon, \beta, \gamma$: constants

2.3 Power fuse

Characteristics of a power fuse are determined by the thermal properties of the metallic material. A logarithmic equation, Eq. (9), with two parameters is used in [7] to model the characteristics of a power fuse, but it is not accurate enough.

$$log(t) = g \times log(x) + h \qquad (9)$$

where

x : fault current
g, h : constants

3. Mathematical Description of ERA

This paper applies the ERA method to identify the state-space equations of the characteristic curves of OC protection devices under modal coordinates. The approach decomposes them into components corresponding to different system eigenvalues or modes. Because the eigenvalues of the system matrix represent the system's natural frequencies, it is easy to use the real and imaginary parts of the eigenvalues to determine the dynamic characteristics of the various components and to isolate the smooth and oscillating components of the characteristic curves of the OC protection devices.

3.1 Description of mathematics concept

For curve fitting, a single input single output (SISO) digital state-space model can be represented by equation [13], and the unit pulse response sequence with zero initial condition is known as the system Markov parameters [12].

The ERA is a technique to identify linear time invariant systems. It produces a state-space description of a physical system from its pulse response sequence. The algorithm has been proven to be efficient and numerically robust to identify the system model. The ERA is based on the Markov parameters as follows:

The system realization is the triplet [A, B, C] [14] computed from the Markov parameters which satisfies the digital state-space model. It begins by forming the generalized $r \times m$ Hankel matrix which is composed of the Markov parameters. Singular Value Decomposition [13] is performed to find $H(0)$ of an appropriate order n, where n is the number of fitting waveform components. Then the identified discrete x (M or fault current) state-space model in the modal coordinates [14] is transformed as follows:

$$x_m(k+1) = \Lambda x_m(k) + B_m u(k) \qquad k = 0,1,2, \dots$$
$$t(k) = C_m x_m(k) + Du(k) \qquad (10)$$

Where Λ is a diagonal matrix containing the eigenvalues λ_i, $i=1,2,\dots n$, of the system, and B_m and C_m are the input and output matrices in the modal coordinates, respectively. The real and imaginary parts of the eigenvalues in Λ are the modal damping rates and natural frequencies, respectively. Once the digital state-space model in the modal coordinates is identified, the OC protection device characteristic curves can be decomposed into various modal components related to the eigenvalues of the identified

state-space matrix.

The above description of ERA mathematics concept was merely applied in [16] to curve-fit the characteristics of EM OC relays. However, in this study the authors apply ERA approach not only to various protective devices but also to obtain an accurate model of multi-type OC protective devices and provides several practical application study cases to fit those accurate characteristic curves.

3.2 Decomposition of the OC protective device characteristic curves

Characteristic curves of the OC protective device are decomposed into various modal components with different exponential constants and different oscillation frequencies determined by the matrix Λ. The digitally recorded OC protective device characteristic curve considered here as the pulse response sequence of the system can be described as follows:

$$t(k) = \begin{cases} Y_0 & k = 0 \\ CE^{k-1}B = C_m \Lambda^{k-1} B_m & k = 1,2,3, \dots \end{cases} \qquad (11)$$

$$t(k) = \sum_{i=1}^{n} c_i \lambda_i^{k-1} b_i \qquad k = 1,2,3, \dots$$
$$= \sum_{i=1}^{n} t_i \qquad (12)$$

Where n is the number of the modal coordinates. The pulse response sequence can then be considered as a combination of n components t_i, $i=1, 2, \dots, n$, that are derived from different modal coordinates.

If the eigenvalue λ_i is real, $\lambda_i = \gamma_i$ and c_i, b_i will also be real, and t_i represents the exponential components as follows:

$$t_i = c_i \gamma_i^{k-1} b_i \qquad k = 1,2,3, \dots \qquad (13)$$

The exponential components which produce the smooth component of the OC protective device characteristic curves are combined as follows:

$$\sum_{i=1}^{n_1} t_i = \sum_{i=1}^{n_1} c_i \lambda_i^{k-1} b_i \qquad k = 1,2,3, \dots \qquad (14)$$

where n_1 is the number of the real eigenvalues.

If the eigenvalues λ_i are complex conjugate pairs

$$\lambda_i = \gamma_i \pm j\omega_i = |z_i| e^{\pm j\theta_i} \qquad (15)$$

c_i, b_i will also be complex conjugates,

$$c_i = |z_{ci}| e^{\pm j\theta_{ci}} \qquad (16)$$
$$b_i = |z_{bi}| e^{\pm j\theta_{bi}} \qquad (17)$$

thus

$$\sum_{i=1}^{n_3} t_i = \sum_{i=1}^{n_3} c_i \lambda_i^{k-1} b_i \qquad k=1,2,3,\ldots$$

$$= \sum_{i=1}^{n_3} |z_{ci}||z_i|^{k-1}|z_{bi}|\cos[(k-1)\theta_i + \theta_{ci} + \theta_{bi}] \qquad (18)$$

Where n_3 is the number of complex conjugate eigenvalue pairs and $n=n_1+n_3$. The sequence t_i represents an oscillation component with oscillation frequency f_i and amplitude attenuation ratio A_{ri} as follows

$$f_i = \theta_i / (2\pi \cdot \Delta x) \qquad (19)$$

$$A_{ri} = V_{p1}/V_{p2} = |z_i|^{-2\pi/\theta_i} \qquad (20)$$

where

Δx : sampling interval
V_{p1} : the first oscillation peak value
V_{p2} : the second peak value

The OC protective device characteristic curves can be represented as

$$t(k) = \sum_{i=1}^{n} t_i$$

$$= \sum_{i=1}^{n_1} c_i \gamma_i^{k-1} b_i \qquad k=1,2,3,\ldots$$

$$+ \sum_{i=1}^{n_2} |z_{ci}||z_i|^{k-1}|z_{bi}|\cos[(k-1)\theta_i + \theta_{ci} + \theta_{bi}] \qquad (21)$$

$$+ \sum_{i=n_2+1}^{2n_2} |z_{ci}||z_i|^{k-1}|z_{bi}|\cos[(k-1)\theta_i + \theta_{ci} + \theta_{bi}]$$

$$+ \sum_{i=2n_2+1}^{n_3} |z_{ci}||z_i|^{k-1}|z_{bi}|\cos[(k-1)\theta_i + \theta_{ci} + \theta_{bi}]$$

which can be expressed in the continuous x domain with a shift x_0 by the following formula [16]:

$$t(x) = \sum_{i=1}^{n_1} C_i e^{-\alpha_i(x-x_0)}$$

$$+ 2\sum_{i=1}^{n_2} K_i A_{ri}^{-f_i(x-x_0)} \cos(2\pi f_i(x-x_0) + \varphi_i) \qquad (22)$$

$$+ \sum_{i=2n_2+1}^{n_3} K_i A_{ri}^{-f_i(x-x_0)} \cos(2\pi f_i(x-x_0) + \varphi_i)$$

where

$$C_i = c_i b_i e^{\alpha_i \Delta x} \qquad i=1,2,3,\ldots n_1 \qquad (23)$$

$$K_i = |z_{ci}||z_{bi}| A_{ri}^{f_i \Delta x} \qquad i=1,2,3,\ldots n_3 \qquad (24)$$

$$\varphi_i = \theta_{ci} + \theta_{bi} - 2\pi f_i \Delta x \qquad i=1,2,3,\ldots n_3 \qquad (25)$$

and

x : M or fault current in the OC protective device characteristic curves
x_0 : *the* value of the sample point one $\triangle x$ to the left of the starting point of the OC protective device characteristic curves
t : OC protective device operating time
n_1 : number of the smooth components
n_2 : *number* of the paired oscillation components (thus the coefficient 2). Since the fitting curves are piecewise nonlinear continuous smooth descending on a log-log coordinates, they produce a lot of paired oscillation components and reduce the number of parameters in Eq. (22)
$(n_3$-$2n_2)$: number of unpaired oscillation components

The characteristic curves of an OC protective device of any type can be represented by a discrete state space model, and the desired bound of the maximum absolute value of errors may be established by selecting an appropriate system model order n.

4. Case Studies

There are five cases with a total number of 19 characteristic curves to be curve-fitted in this study. Four types of typical OC protective devices and two types of non-typical OC protective devices used are studied to validate the adaptability of the proposed fitting method: four EM OC relays with *TDS*=2 [8, 17], three IEEE normal standard digital OC relays with *TDS*=1 [5], four IEC normal standard digital OC relays with *TDS*=1 [15, 21], two power fuses with 50A and 80A [18], and two OC protective devices with specific desired characteristics and four protective OC devices with fixed slope characteristics. For both accuracy and reason considerations, the constraint for the fit is that the maximum absolute values of errors of all the fitted points of the characteristic curves be less than 10 milliseconds.

4.1 Case (1): EM OC relays

Four ABB inverse-time EM OC relays with *TDS*=2 are chosen: CO2 (short inverse), CO6 (definite inverse), CR8 (inverse) and CO11 (extremely inverse). Their codes are CO2-s_2, CO6-d_2, CR8-i_2 and CO11-e_2, respectively.

The values of the parameters in Eq. (22) are listed in Table 1, and the actual characteristic curves and the fitting curves are shown in Fig. 2. The absolute values of errors for the 486 sample points of the CR8 relay are plotted in Fig. 3.

4.2 Case (2): IEEE standard digital OC relay

Eq. (7) is used as the formula for three types of IEEE digital OC relays: moderately inverse, very inverse, and

Table 1. The parameters in Eq. (22) for the fitting curves of the ABB inverse-time EM OC relays

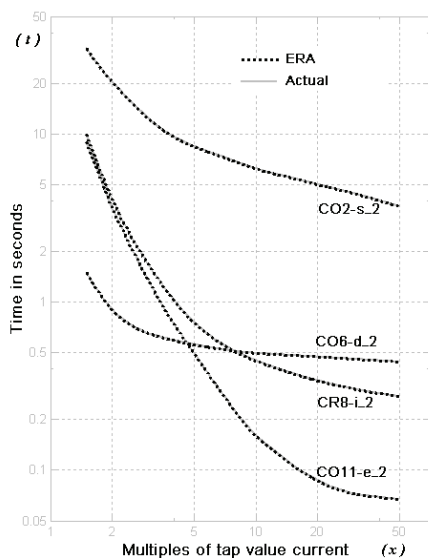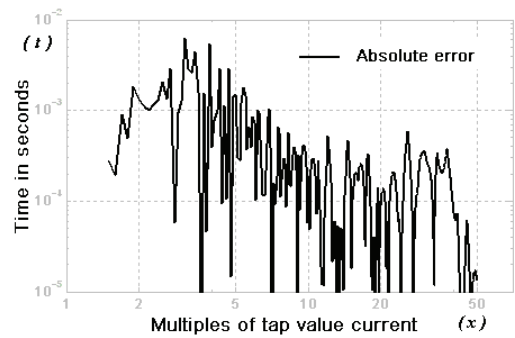| Protective Devices	ABB's CO2 relay	ABB's CO6 relay	ABB's CR8 relay	ABB's CO11 relay
Types	short	definitely	inverse	extremely
Codes	CO2-s_2	CO6-d_2	CR8-i_2	CO11-e_2
C_1	6.1462E+00	8.5304E-01	6.4064E+00	8.1916E+00
α_1	6.4903E+00	3.2740E+00	4.0563E+00	3.4719E+00
C_2	2.2066E+01	3.9380E-01	2.8572E+00	3.1651E+00
α_2	1.1386E+00	5.9051E-01	1.6897E+00	7.1558E-01
C_3	4.1210E+00	4.6640E-01	2.9571E+00	3.5151E-01
α_3	2.1050E-01	1.3022E-03	7.6835E-01	1.6352E-01
C_4	3.2493E+00	6.0030E-02	3.2644E-01	7.1651E-02
α_4	2.1554E-03	6.8302E-02	3.6731E-03	-9.4391E-04
C_5	3.0397E+00	-	3.8298E-01	-1.4976E-03
α_5	2.8129E-02	-	1.2661E-01	-3.5852E-02
K_1	3.7010E-01	2.1649E-02	2.1199E-03	7.0326E-02
f_1	9.7370E-02	1.4677E-01	4.0621E-02	1.5807E-01
A_{r1}	1.8696E+01	2.5197E+01	6.1212E+00	2.2947E+01
φ_1	-3.0681E+00	1.4085E+00	-3.3639E-01	5.8185E-01
K_2	-	4.5547E-03	3.3388E-02	1.5734E-01
f_2	-	3.1066E-01	1.1768E-01	3.3774E-01
A_{r2}	-	3.8163E+00	3.8805E+01	2.5583E+01
φ_2	-	4.2344E-01	2.1498E+00	-1.8850E+00
K_3	-	-	6.1299E-02	1.0803E-01
f_3	-	-	4.3718E+00	2.0367E+00
A_{r3}	-	-	1.7453E+00	4.7568E+00
φ_3	-	-	-2.8635E-01	1.4746E+00
K_4	-	-	-	5.9913E-02
f_4	-	-	-	4.0781E+00
A_{r4}	-	-	-	2.2643E+00
φ_4	-	-	-	2.6033E-01
K_9	-	2.1242E-02	6.5679E-02	-
f_9	-	5.0000E+00	5.0000E+00	-
A_{r9}	-	2.7027E+00	8.2764E+00	-
φ_9	-	0.0000E+00	0.0000E+00	-

Fig. 3. Absolute values of errors for the CR8 relay with **TDS=2.**

Table 2. The parameters in Eq. (22) for the fitting curves of the IEEE digital OC relays

Protective Devices	IEEE digital OC relay	IEEE digital OC relay	IEEE digital OC relay
Types	moderately	very	Extremely
Codes	IEEE-m_1	IEEE-v_1	IEEE-e_1
C_1	2.2102E+00	4.2242E+00	6.0467E+00
α_1	4.5627E+00	6.6735E+00	6.6941E+00
C_2	2.4813E+00	7.9414E+00	1.1407E+01
α_2	1.4290E+00	2.7114E+00	2.7203E+00
C_3	1.3367E+00	5.6281E+00	8.1096E+00
α_3	4.2206E-01	1.1127E+00	1.1176E+00
C_4	9.0850E-01	2.0752E+00	3.0034E+00
α_4	4.1790E-03	4.3402E-01	4.3684E-01
C_5	7.0080E-01	5.1460E-01	1.5763E-01
α_5	1.0101E-01	6.6090E-04	3.6082E-03
C_6	-	4.2450E-01	6.1905E-01
α_6	-	1.4023E-01	1.4191E-01

extremely inverse. The values of *TDS*, β, γ and ε for these three relays in Eq. (7) are 1.0, 0.0515, 0.0200 and 0.1140, 1.0, 19.61, 2.0000 and 0.4910, and 1.0, 28.2, 2.000, and 0.1217, respectively. Their codes are IEEE-m_1, IEEE-v_1 and IEEE-e_1, respectively.

The values of the parameters in Eq. (22) are listed in Table 2, and the actual characteristic curves and the fitting curves are shown in Fig. 4.

4.3 Case (3): IEC standard digital OC relay

Eq. (8) is used as the formula for four types of ABB's SPAJ140C digital OC relays: long-time inverse, normal inverse, very inverse, and extremely inverse. The values of *TDS*, β, and γ for these four relays in Eq. (8) are 1.0, 120 and 1.0, 1.0, 0.14 and 0.02, 1.0, 13.5 and 1.0, and 1.0, 80.0 and 2.0, respectively. Their codes are IEC-l_1, IEC-n_1, IEC-v_1 and IEC-e_1, respectively.

The values of the parameters in Eq. (22) are listed in Table 3, and the actual characteristic curves and the fitting curves are shown in Fig. 5.
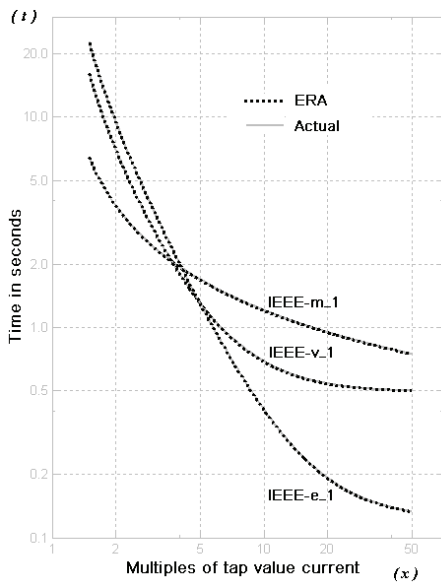

Fig. 2. The actual characteristic curves and the fitting curves for the four ABB inverse-time EM OC relays with **TDS=2.**

Fig. 4. The actual characteristic curves and the fitting curves for the three IEEE digital OC relays with **TDS=1.0.**
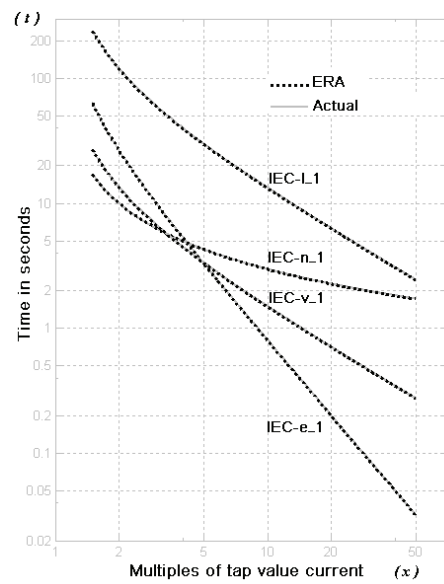

Fig. 5. The actual characteristic curves and the fitting curves for the four IEC digital OC relays with **TDS=1.0.**

Table 3. The parameters in Eq. (22) for the fitting curves of the four IEC digital OC relays

Protective Devices Types	IEC digital OC relay long-time	IEC digital OC relay normal	IEC digital OC relay very	IEC digital OC relay Extremely
Codes	IEC-l_1	IEC-n_1	IEC-v_1	IEC-e_1
C_1	3.5702E+01	3.7947E+00	6.6067E+00	1.5547E+01
α_1	7.7521E+00	5.9976E+00	6.3078E+00	6.9822E+00
C_2	8.4519E+01	6.2397E+00	1.1609E+01	3.1247E+01
α_2	3.4123E+00	2.2685E+00	2.4609E+00	2.9059E+00
C_3	8.1361E+01	4.4653E+00	8.4898E+00	2.3884E+01
α_3	1.5144E+00	8.4487E-01	9.5445E-01	1.2264E+00
C_4	5.1951E+01	2.5127E+00	4.3242E+00	9.7140E+00
α_4	6.5615E-01	2.9285E-01	3.5104E-01	4.9965E-01
C_5	2.7600E+01	2.0492E+00	6.4559E-01	2.2992E+00
α_5	2.6688E-01	3.9934E-03	1.8220E-02	1.7998E-01
C_6	4.8669E+00	1.5567E+00	1.8904E+00	2.7211E-01
α_6	1.5574E-02	7.9565E-02	1.0994E-01	4.4719E-02
C_7	1.3277E+01	-	-	-
α_7	9.0201E-02	-	-	-

4.4 Case (4): Two power fuses and two non-typical OC protective devices with specific characteristic curves

Two similar extremely inverse-time current-limiting power fuses, SIBA 6/12kV 50A and 80A, and two non-typical OC protective devices with curves drawn by the engineer to avoid passing through specific points are selected to be fitted. Their codes are PF-e_50 and PF-e_80, and SFC_1 and SFC_2, respectively.

The values of the parameters in Eq. (22) are listed in Table 4, and the actual characteristic curves and the fitting curves are shown in Fig. 6.

Table 4. The parameters in Eq. (22) for the fitting curves of the two power fuses and two non-typical OC protective devices with specific characteristic curves

Protective devices	SIBA 50A	SIBA 80A	Specified OC relay	Specified OC relay
Types	similar extremely	similar extremely	-	-
Codes	PF-e_50	PF-e_80	SFC_1	SFC_2
C_1	1.3265E+03	-6.7027E-01	1.5905E+01	1.7252E+03
α_1	6.6117E+00	8.3182E-01	5.1571E-01	1.8506E+00
C_2	1.8880E+01	6.7912E+01	4.0231E-02	3.3349E+01
α_2	9.4762E-02	4.7583E-02	3.2646E-02	1.4955E-01
C_3	7.4639E+01	1.1043E+02	-	-
α_3	6.1627E-02	2.2943E-02	-	-
C_4	7.3882E+01	1.2697E+01	-	-
α_4	3.8179E-02	1.1087E-02	-	-
C_5	1.5433E+01	3.3351E-01	-	-
α_5	2.1579E-02	3.3167E-03	-	-
C_6	4.3597E-01	-	-	-
α_6	8.1541E-03	-	-	-
K_1	5.5714E-03	3.6269E-01	6.1591E+00	8.1807E+00
f_1	9.2321E-03	3.9288E-03	1.2184E-01	1.6486E-02
A_{r1}	2.1573E+00	1.9038E+01	1.3381E+02	2.6779E+03
φ_1	6.1321E-01	2.7626E-01	1.2778E+00	2.7279E+00
K_2	8.5067E-04	3.6332E-01	9.6143E-01	7.5485E+02
f_2	1.7877E-02	6.0723E-03	2.4185E-01	2.4643E-01
A_{r2}	1.2638E+00	1.8093E+01	6.6413E+00	3.2966E+03
φ_2	-1.6870E+00	-5.8911E+00	2.1739E+00	2.7173E+00
K_3	2.6661E-04	7.5234E-03	5.7320E+02	5.3106E+01
f_3	2.5101E-02	8.8610E-03	9.8632E-01	8.1740E-01
A_{r3}	1.1137E+00	2.0836E+00	3.1281E+05	6.5326E+00
φ_3	-2.5755E+00	-5.0891E+00	-1.8269E+00	-2.2071E+00
K_4	-	2.6936E-03	6.6925E+01	8.0408E+00
f_4	-	1.2075E-02	3.5083E+00	1.3857E+00
A_{r4}	-	1.5736E+00	1.9791E+01	2.1467E+00

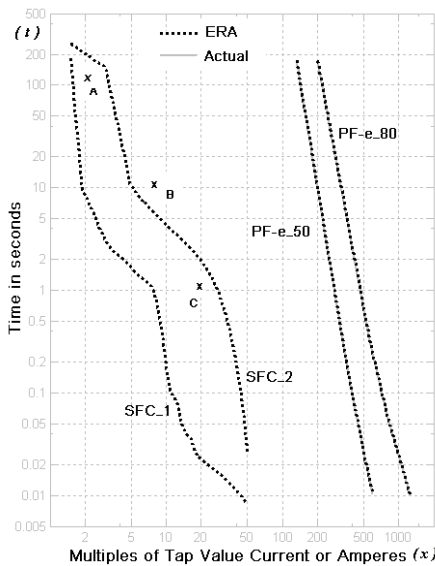|				
φ_4	-	2.0512E-01	-2.0732E+00	-1.4969E+00
K_5	-	4.8919E-04	-	-
f_5	-	1.6183E-02	-	-
A_{r5}	-	1.2430E+00	-	-
φ_5	-	3.8113E+00	-	-
K_6	-	1.0698E-03	-	-
f_6	-	1.8122E-02	-	-
A_{r6}	-	1.4469E+00	-	-
φ_6	-	-1.1383E+00	-	-

Fig. 6. The actual characteristic curves and the fitting curves for the two power fuses and the two non-typical OC protective devices with specific characteristic curves.

Table 5. The parameters in Eq. (22) for the fitting curves of the four non-typical OC protective devices with fixed slope characteristic curves

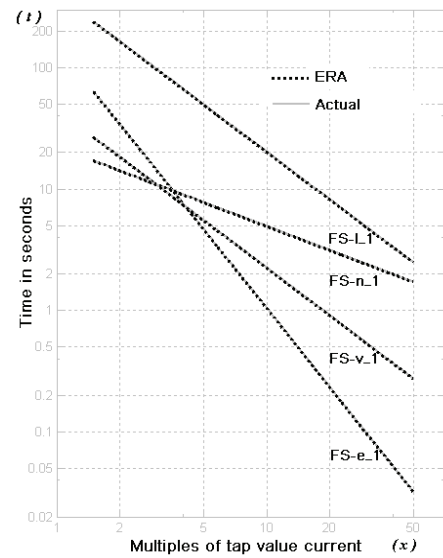| Protective devices	Fixed Slope OC relay	Fixed Slope OC relay	Fixed Slope OC relay	Fixed Slope OC relay
Type	long-time	normal	very	Extremely
Codes	FS-l_1	FS-n_1	FS-v_1	FS-e_1
C_1	1.0379E+01	1.7910E+00	5.2458E+00	9.0532E+00
α_1	3.6629E+00	1.8681E+00	2.3769E+00	3.8174E+00
C_2	5.0499E+01	4.6572E+00	1.1559E+01	2.8638E+01
α_2	1.8535E+00	7.1011E-01	9.6036E-01	1.8740E+00
C_3	7.6542E+01	4.9432E+00	8.3249E+00	2.4412E+01
α_3	9.4609E-01	2.6227E-01	3.7208E-01	9.0196E-01
C_4	6.4004E+01	2.6605E+00	8.7979E-01	9.7140E+00
α_4	4.6863E-01	9.9747E-03	2.4567E-02	4.0528E-01
C_5	3.8298E+01	3.9250E+00	3.5017E+00	2.2253E+00
α_5	2.1527E-01	7.9644E-02	1.2410E-01	1.5861E-01
C_6	5.0562E+00	-	-	2.5012E-01
α_6	1.7446E-02	-	-	4.3046E-02
C_7	1.7757E+01			
α_7	8.1868E-02			

Fig. 7. The actual characteristic curves and the fitting curves for the four non-typical OC protective devices with fixed slope characteristic curves.

4.5 Case (5): Four non-typical OC protective devices with fixed slope characteristic curves

Four non-typical OC protective devices with fixed slope curves on a log-log coordinates are chosen. Their starting points (M_1, t_1) and end points (M_2, t_2) are the same as those of the IEC digital OC relays in case (3): (1.5, 240.00000) and (50, 2.44900), (1.5, 17.19400) and (50.0, 1.7203), (1.5, 27.00000) and (50.0, 0.27551), and (1.5, 64.00000) and (50, 0.032103), respectively. Their codes are FS-l_1, FS-n_1, FS-v_1 and FS-e_1, respectively.

The values of the parameters in Eq. (22) are listed in Table 5, and the actual characteristic curves and the fitting curves are shown in Fig. 7.

5. Results Analysis

19 characteristic curves are fitted by the proposed ERA method. The results and its practical applications in power systems are analyzed and discussed below:

5.1 Simulation results analysis

As can be seen in Fig. 2 and Figs. 4-7, the curves obtained by Eq. (22) from the ERA method and the actual characteristic curves are so closely matched that they are virtually indistinguishable, for all types of OC protective devices. This clearly demonstrates the accuracy and identification robustness of the ERA method.

The absolute values of errors for the 486 sample points of the CR8 relay with *TDS*=2 are plotted in Fig. 3. As can be seen in this Fig, the absolute values of errors are within

Table 6. The specifications and partial results of Eq. (22) for the 19 characteristic curves

No.	Codes	l_s	X	Δx	x_0	x_1	n	n_1	n_2	n_3-2n_2	n_3-n_2
1	CO2-s_2	487	1.5-50	0.1	1.4	1.5	7	5	1	0	1
2	CO6-d_2	487	1.5-50	0.1	1.4	1.5	9	4	2	1	3
3	CR8-i_2	487	1.5-50	0.1	1.4	1.5	12	5	3	1	4
4	CO11-e_2	487	1.5-50	0.1	1.4	1.5	13	5	4	0	4
5	IEEE-m_1	487	1.5-50	0.1	1.4	1.5	5	5	0	0	0
6	IEEE-v_1	487	1.5-50	0.1	1.4	1.5	6	6	0	0	0
7	IEEE-e_1	487	1.5-50	0.1	1.4	1.5	6	6	0	0	0
8	IEC-l_1	487	1.5-50	0.1	1.4	1.5	7	7	0	0	0
9	IEC-n_1	487	1.5-50	0.1	1.4	1.5	6	6	0	0	0
10	IEC-v_1	487	1.5-50	0.1	1.4	1.5	6	6	0	0	0
11	IEC-e_1	487	1.5-50	0.1	1.4	1.5	6	6	0	0	0
12	PF-e_50	468	133-599	1	132	133	12	6	3	0	3
13	PF-e_80	356	201-1263	3	198	132	17	5	6	0	6
14	SFC_1	487	1.5-50	0.1	1.4	1.5	10	2	4	0	4
15	SFC_2	487	1.5-50	0.1	1.4	1.5	10	2	4	0	4
16	FS-l_1	487	1.5-50	0.1	1.4	1.5	7	7	0	0	0
17	FS-n_1	487	1.5-50	0.1	1.4	1.5	5	5	0	0	0
18	FS-v_1	487	1.5-50	0.1	1.4	1.5	5	5	0	0	0
19	FS-e_1	487	1.5-50	0.1	1.4	1.5	6	6	0	0	0

Table 7. Summary of the errors of the fitting of the 19 characteristic curves

No.	Codes	Max_Err/x	Max_Err%/x	AV	AV%
1	CO2-s_2	6.24/1.9	0.09/20.0	0.91	0.16
2	CO6-d_2	6.10/2.5	0.84/2.5	0.17	0.03
3	CR8-i_2	6.20/3.1	0.50/3.9	0.27	0.05
4	CO11-e_2	8.26/3.5	1.19/16.2	0.44	0.32
5	IEEE-m_1	7.91/1.6	0.14/1.6	0.61	0.06
6	IEEE-v_1	2.42/1.6	0.06/41.7	0.21	0.03
7	IEEE-e_1	3.26/1.6	0.30/41.6	0.29	0.12
8	IEC-l_1	9.77/1.7	0.04/45.5	0.83	0.01
9	IEC-n_1	3.94/1.6	0.03/45.5	0.33	0.01
10	IEC-v_1	5.61/1.6	0.20/43.6	0.45	0.07
11	IEC-e_1	6.71/1.6	2.13/49.9	0.57	0.45
12	PF-e_50	3.18/299	5.24/547	0.51	0.94
13	PF-e_80	4.55/204	1.53/1248	0.31	0.23
14	SFC_1	-	-	-	-
15	SFC_2	-	-	-	-
16	FS-l_1	1.42/1.9	0.02/46.9	0.20	0.01
17	FS-n_1	3.28/1.5	0.03/45.1	0.41	0.01
18	FS-v_1	6.42/1.5	0.33/42.5	0.78	0.11
19	FS-e_1	1.91/1.9	0.72/50.0	0.22	0.18

the constraint range, with larger values corresponding to smaller values of x. This result shows that it is more difficult to fit the characteristic curves where the protective device operating time changes nonlinearly and drastically, as already stated in Section 1.

The specifications and partial results of the 19 characteristic curves by the proposed ERA method are shown in Table 6. The specifications are the same for the 11 typical OC protective devices and 6 non-typical OC protective devices, but are different for the two power fuses. As a result, there are three types of data sequences. The numbers of sampling points l_s are 487, 468 and 356. The range of x (M or fault current) of the characteristic curves of the OC protective devices are 1.5-50.0, 133-599 and 201-1263, and the sampling intervals $\triangle x$ are 0.1, 1 and 3, respectively. The values of x_0 of the sample points one $\triangle x$ to the left of the starting points of the OC protective devices characteristic curves are 1.4, 132 and 198, respectively. The values of x_1 of the starting sample points at the left of the OC protective devices characteristic curves are 1.5, 133 and 132, respectively. The numbers of the fitting components (n) are set to 5-17, with the numbers of smooth components (n_1) 2-7, the numbers of double (paired) oscillation components (n_2) 0-6, the numbers of single (unpaired) oscillation components (n_3-2n_2) 0-1, and the total numbers of different oscillation components (n_3-n_2) 0-6.

Some unique properties of the results are discussed below.
(1) The characteristic curves of two of the devices fitted by Eq. (22), CO6-d_2 and CR8-i_2, consist of only 1 (n_3-2n_2) unpaired oscillatory components. The number of parameters in Eq. (22) is much less for such types of devices, as stated in Section Ⅲ.
(2) As shown in case (1), 7-13 curve-fitting components are needed for the various types of EM OC relays, and

more components are needed to fit relays with more inverse-time characteristics to achieve the same level of maximum absolute values of errors.
(3) As shown in case (3) for the four IEC digital OC relays and in *case* (5) for the four non-typical OC protective devices, more components are needed to fit relays with long-time inverse characteristics to achieve the same level of maximum absolute values of errors.
(4) The powe*r* fuses in case (4) is more extremely inverse than regular relays and they are similar to long-time inverse relays. As a result, up to 17 components are needed to fit the curves of the power fuses.
(5) Because the formulas of the characteristics of the digital OC relays in case (2) and (3) are exponential in nature, there are only smooth components but no oscillatory components in the fitting curves, as shown in Table 6 from Eq. (22). The same happens in case (5) for devices with fixed slope curves.

The four types of errors of the fitting of the 19 characteristic curves are summarized in Table 7. The range of the maximum absolute values of errors (Max_Err) is 1.42-9.77 ms, and all occur at smaller x values (i.e., 1.5-3.5, 299 and 204). The range of the maximum absolute values of percentage errors (Max_Err%) is 0.02-5.24, and more than two-third of them occur at larger values of x (i.e., 41.6-50.0, 547 and 1248). Larger x values correspond to smaller operating times. The range of the averages of absolute values of errors (AV) is 0.17-0.91 ms, and the range of the averages of absolute values of percentage errors (AV%) is 0.01-0.94.

The fact that all of the fitting errors are well within the constraint range indicates that the proposed ERA method is accurate enough to fit characteristic curves for all practical purposes. However, more fitted components can be chosen

if greater precision is desired. Although the maximum absolute values of errors occur mostly at small x values where the protective device operating times are highly nonlinear and changes rapidly, the curves fitted by ERA can still match the OC protective device characteristic very closely.

With reference to Table 6, set the maximum values for the numbers of smooth components n_1 and the total numbers of different oscillation components n_3-n_2 to 7 and 6, respectively, and change the parameter K_i to N_i in Eq. (22), Eq. (22) may be rewritten as Eq. (26). Eq. (26) is a versatile formula which can fit not only the 19 curves in this study but also most of the curves which are nonlinear piecewise continuous smooth descending on a log-log coordinates. With its 38 parameters, Eq. (26) can accurately fit characteristic curves of all OC protective devices in power systems.

$$t(x) = \sum_{i=1}^{7} C_i e^{-\alpha_i(x-x_0)}$$
$$+ \sum_{i=1}^{6} N_i A_{r_i}^{-f_i(x-x_0)} \cos(2\pi f_i(x-x_0) + \varphi_i) \qquad (26)$$

6. Practical Applications

Eq. (26), which comprises of 7 smooth components and 6 oscillatory components, may be adopted as the model of a novel flexible OC relay which can be used to solve protective coordination problems in power systems. The benefits are described below:

(1) Eq. (26) can fit non-typical OC protective devices, e.g., SFC_1 and SFC_2 in Fig. 6 and FS-l_1, FS-n_1, FS-v_1 and FS-e_1 in Fig. 7, as well as typical OC protective devices. Any device can be fitted by simply changing the values of the parameters in Eq. (26).
(2) The existing EM OC relays and digital OC relays can be easily replaced by the novel flexible OC relays if a device failure happens or system reconfiguration is needed. The novel flexible OC relays are very flexible and can easily adapt to various system configurations.
(3) The characteristic of a novel flexible OC relay can be modified or reprogrammed easily when the load changes or when it is relocated or reassigned to different tasks.
(4) For utilities that must follow the government purchase law such as the Taipower Company in Taiwan, no devices from the same manufacturer may be purchased at all times, and this often leads to troubles in protective coordination. However, if novel flexible OC relays are purchased instead, they will be able to provide excellent coordination with either upstream or downstream protective devices in almost all circumstances.
(5) As shown in Fig. 6, the S-shape SFC_2 characteristic curve of the novel flexible OC relay can be programmed

to avoid passing through specific points such as A, B and C. This technique can be applied to protect a transformer, e.g., the characteristic curve must lie between the ANSI point and the in-rush current and its starting point should be less than 6 times the rated current of the transformer. As also shown in Fig. 6, the SFC_1 characteristic curve is an opposite S-shape curve, which demonstrates even more the flexibility of the relay.
(6) A single versatile formula, Eq. (26), may be used to represent the characteristics of the EM OC relays and power fuses by the manufactures.
(7) Because the characteristics of typical OC protective devices can be represented by Eq. (26), human errors such as misjudgments of the coordinates of a curve crossover can be avoided, and the CTI (coordination time interval) values between the upstream and downstream protective devices for all fault currents can be determined accurately.
(8) Microgrid systems have drawn much attention in recent years. The fault currents differ tremendously between an isolated island grid and a connected grid, which makes protective coordination in microgrid systems very difficult. The novel flexible OC relay can provide different characteristic curves to be used in different system configurations to solve protective coordination problems in different situations.

7. Conclusions

This paper proposes ERA method to determine a multi-type practical OC protective device models and their practical applications to fit accurate characteristic curves. The discrete state space model with appropriate system order can fit characteristics curves of all types of OC protective devices. The characteristic curves are decomposed by the ERA method into various smooth and oscillatory modal components and are represented by a single versatile formula that greatly facilitates further analysis and design. 19 characteristic curves from 13 typical OC protective devices and 6 non-typical OC protective devices are chosen for curve-fitting, and the results are all excellent. Simulation results of this study demonstrate that the proposed ERA method is not only an analytical tool in modeling OC protective devices and determining the parameters in the fitting equations, but also a practical tool for solving OC protection problems.

The characteristics of the existing OC protective devices in the sub-transmission and distribution systems are all piecewise nonlinear continuous smooth curves on a log-log coordinates. Therefore, the characteristic curves of any of such devices can be fitted accurately by the versatile formula derived by the proposed ERA method, and a novel flexible OC relay modeled by this versatile formula can be installed in almost all system configurations as a customized OC relay to meet various requirements. The proposed new

type of OC relay not only is more flexible and adaptable but also improves the overall OC protective coordination in the sub-transmission and distribution systems.

References

[1] Conde, E. Vazquez, Application of a proposed overcurrent relay in radial distribution networks, *Electric Power Systems Research*, Vol. 81, No. 2, February 2011, pp. 570-579.

[2] M.S. Sachdev, J. Singh, R. J. Fleming, Mathematical Models Representing Time-Current Characteristics of Overcurrent Relays for Computer Applications, IEEE PES Paper No. A78-131-5 Winter meeting, January 1978.

[3] IEEE Committee Report, Computer representation of overcurrent relay characteristics, *IEEE Transactions on Power Delivery*, Vol. 4, No. 3, July 1989, pp. 1659-1667.

[4] S. Chan, R. Maurer**,** Modeling Overcurrent Relay Characteristics, *IEEE Computer Applications in Power*, Vol. 5, No. 1, 1992, pp. 41-45.

[5] IEEE PSRC Committee, IEEE Standard Inverse-Time Characteristic Equations for Overcurrent Relays, *IEEE Transactoions on Power* Delivery, Vol.14, No.3, July 1999, pp.868-872.

[6] H.K. Karegar, H.A. Abyaneh, M. Al-Dabbagh, A flexible approach for overcurrent relay characteristics simulation, *Electric Power Systems Research*, Vol.66, No.3, September 2003, pp.233-239.

[7] S. Chaitusaney, A. Yokoyama, Prevention of Reliability Degradation from Reclose-Fuse Miscoordi-nation Due to Distributed Generation, *IEEE Transactions on Power Delivery*, Vol. 23, No. 4, October 2008, pp. 2545-2554.

[8] T.H. Tan, G.H. Tzeng, Industry Power Distribution, 4th ed., *Gau Lih Book Co.*, Taiwan, ISBN: 978-957-58-4133-1, pp.223-229, 2011.

[9] M. Geethanjali, S.M.R. Slochanal, A combined adaptive network and fuzzy inference system (ANFIS) approach for overcurrent relay system, *NEURO-COMPUTING*, Vol. 71, No. 4-6, January 2008, pp. 895-903.

[10] Arturo Conde Enríquez, Ernesto Vázquez-Martínez, Héctor J. Altuve-Ferrer, Time overcurrent adaptive relay, *Electrical Power and Energy Systems*, Vol. 25, No. 10, December 2003, pp. 841-847.

[11] H. A. Darwish, M. A. Rahman, A. I. Taalab, H. Shaaban, Digital model of overcurrent relay charac-teristics, *Industry Applications Conference*, Vol. 2, 1995, pp. 1187-1192.

[12] J. Juang, R.S. Pappa, "An eigensystem realization algorithm for modal parameter identification and model reduction", J. Guidance Control, Vol. 8, pp. 620-627, 1985.

[13] J.N. Juang, Applied System Identification, Prentice-Hall, Inc., Englewood Cliffs, New Jersey, USA, 1994.

[14] Z. Ma, S. Ahuja, C.W. Rowley, Reduced-order models for control of fluids using the eigensystem realization algorithm, *Theoretical and Computational Fluid Dynamics,* Vol.25, No.1-4, June 2011, pp.233-247.

[15] IEC Publication 255-3 (1989-05), *Single Input Energizing Quality Measuring Relays with Dependent or Independent*.

[16] Feng-Jih Wu, Chih-Ju Chou, Ying Lu, Jarm-Long Chung, "Modeling Electromechanical Overcurrent Relays Using Singular Value Decomposition," Jou rnal of Applied Mathematics, Volume 2012 (201 2), Article ID 104952, 18 pages

[17] Instruction 41-131Q, Types CR, CRC, CRP and CRD Directional Overcurrent Relays, *ABB Co.* Coral Springs, FL, 1998.

[18] Catalog, High Voltage Fuse acc. DIN Standard, *SIBA Co.*, pp.87

[19] J.C. Tan, P.G. McLaren, R.P. Jayasinghe, P.L. Wilson, Software Model for Inverse Time Overcurrent Relays Incorporating IEC and IEEE Standard Curves, *Proceedings of the 2002 IEEE Canadian Conference on Electrical & Computer Engineering*, Vol.1, 2002, pp. 37-41.

[20] BE1-1051 Manual, Basler Electric Co.

[21] User's Manual and Technical Description, SPCJ4D29 Combined Overccurent and Earth-Fault Relay Module ABB Co. Coral Springs, FL, Jan. 30, 1997.

Chau-Yuan Cheng was born in Chang-Haw, Taiwan. He received his M.S degree from National Taiwan Marine & Ocean University and Taipei University of Technology, respectively. He is an assistant professor at St. John's University since 2008. His research interests in analysis of power system, wind power mill design, electrical machinery, and industrial management. He is a member of measurement association in Taiwan.

Feng-Jih Wu was born in Taiwan, R.O.C., in 1961. He received the M.S. degree in electrical engineering from the National Cheng Kung University in 1987 and the Ph.D. degree in electrical engineering from National Taipei University of Technology in 2013. From 1989 to 2013, He joined the faculty of St.John's University, Taipei, Taiwan, as an instructor. Currently, he is an Associate Professor with the Department of Electrical Engineering, at same university. His major interests are in microgrid relaying protection